Available online at www.sciencedirect.com
SCIENCE DIRECT®
Journal of Sound and Vibration 277 (2004) 783–799
JOURNAL OF SOUND AND VIBRATION
www.elsevier.com/locate/jsvi

Strange attractors and chaos control in a Duffing–Van der Pol oscillator with two external periodic forces

F.M. Moukam Kakmeni[a,*], S. Bowong[b], C. Tchawoua[a], E. Kaptouom[c]

[a] *Laboratoire de Mécanique, Département de Physique, Faculté des Sciences, Université de Yaoundé I, B.P. 812 Yaoundé, Cameroun, France*

[b] *INRIA Lorraine, Projet Conge & University of Metz, I.S.G.M.P., Bât A, 57045 Metz Cedex 01, France*

[c] *Ecole Nationale Supérieure Polytechnique, Université de Yaoundé I, B.P. 8390 Yaoundé, Cameroun, France*

Received 7 October 2002; accepted 8 September 2003

Abstract

An anharmonic Duffing–Van der Pol oscillator with two external forces is considered. By applying numerical results, strange attractors are presented and the chaotic behaviour is investigated. The problem of directing a chaotic state of the system to a periodic orbit is studied. By assuming that the exact model of the system is not known and that the position is the only state available for measurements, the controller comprises a linearizing-like feedback and an estimator. Simulations are provided to illustrate the performance of the controller.

1. Introduction

Research in the area of non-linear oscillators of various types has received a great deal of attention in recent years. Prominent among them is the Duffing–Van der Pol (DVP) oscillator, described by the equation

$$\ddot{x} - \mu(1 - x^2)\dot{x} + \omega_0^2 x + \lambda x^3 = U(t), \tag{1}$$

where μ, ω_0, λ are constant parameters and $U(t)$ is an external force. This non-linear differential equation is used in physics, engineering, electronics, biology, neurology and many other disciplines [1–8]. It is therefore one of the most intensively studied systems in non-linear dynamics [1,7].

*Corresponding author. Tel.: +237-976-22-29.

E-mail addresses: fmoukam@uycdc.uninet.cm (F.M. Moukam Kakmeni), sbowong@uycdc.uninet.cm (S. Bowong), ctchawoua@uycdc.uninet.cm (C. Tchawoua).

0022-460X/$ - see front matter
doi:10.1016/j.jsv.2003.09.051

In the presence of an external periodic force (e.g. $U(t) = U_0 \cos \omega t$) the DVP oscillator shows hysteresis, multistability, period doubling, intermittent transitions to chaos, local bifurcation and strange attractor phenomena [5,6].

Less effort has been devoted to the case where the external force has more than one periodic component. One can mention the work of Yagasaki who studied chaotic motion near homoclinic manifolds and resonant toris [9], and homoclinic motions and chaos in the quasiperiodically forced DVP oscillator with single well potential [10].

On the other hand, since the pioneering work of Ott et al. [11] who used small parameter perturbations to stabilize a saddle fixed or periodic point contained in a chaotic attractor, the control of chaotic systems has become a challenging problem of intrinsic interdisciplinary interest. One motivation for such research is their obvious importance in relation to applications. For example, controlling the chaotic brain wave of the human being "may be chief property that makes the brain different from an artificial-intelligence machine" [12]. Different types of control phenomena have been observed in variety of chaotic systems. The occurrence of a particular type of control may depend on the structure of the underlying dynamical system considered [8,13–16].

In this paper, the dynamics and chaos control of the DVP oscillator (1) subjected to two periodic external forces are investigated; that is,

$$U(t) = f \cos(vt + \alpha) + g \cos(\omega t + \beta), \tag{2}$$

where f, g, α, β, v and ω are constants.

In Section 2 by applying computational methods, bifurcation diagrams, Poincaré maps and Lyapunov exponents are presented to observe periodic and chaotic motions. In Section 3, a linearizing-like control scheme is applied to drive the chaotic state of the DVP oscillator to one of its periodic orbits. It is assumed that uncertainties in the model are present. That is, the robust stabilization problem of chaotic signals against model uncertainties is addressed. The paper ends with conclusion in Section 4.

2. Chaotic state

An interesting question related to the problem of chaos is the way the chaos appears in the system. In this section, numerical studies have been done with a view to finding the sensitivity and some sets of parameters which lead to chaotic behaviour. The following bifurcation diagrams (Figs. 1(a) and (b)) have been drawn showing transition to chaos for $\mu = 0.2$, $\omega_0 = 1$, $f = 0.48$, $v = 1$, $\omega = 3$ and $\alpha = \beta = 0$.

In Fig. 1(a) the bifurcation diagram shows the amplitude of the oscillation in the Poincaré cross-section versus the amplitude of the second external force g for $\lambda = 0.8$. Periodic, quasiperiodic and chaotic oscillations are clearly visible in the figure. In fact, for small values of g ($0 < g < 1.75$) the system's behaviour is fundamentally quasiperiodic. However, a very short interval of periodicity is located at approximately $g = 1.5$. When g is increased right above the value 1.75, the system jumps into a stable regular state characterized by periodic motions of a relatively long period. As g continues to be increased, these periodic states undergo period-doubling bifurcations that lead the system into another chaotic state. This latter behaviour ceases abruptly at $g = 4$, giving place to periodic motions, yet with relatively short periods as compared

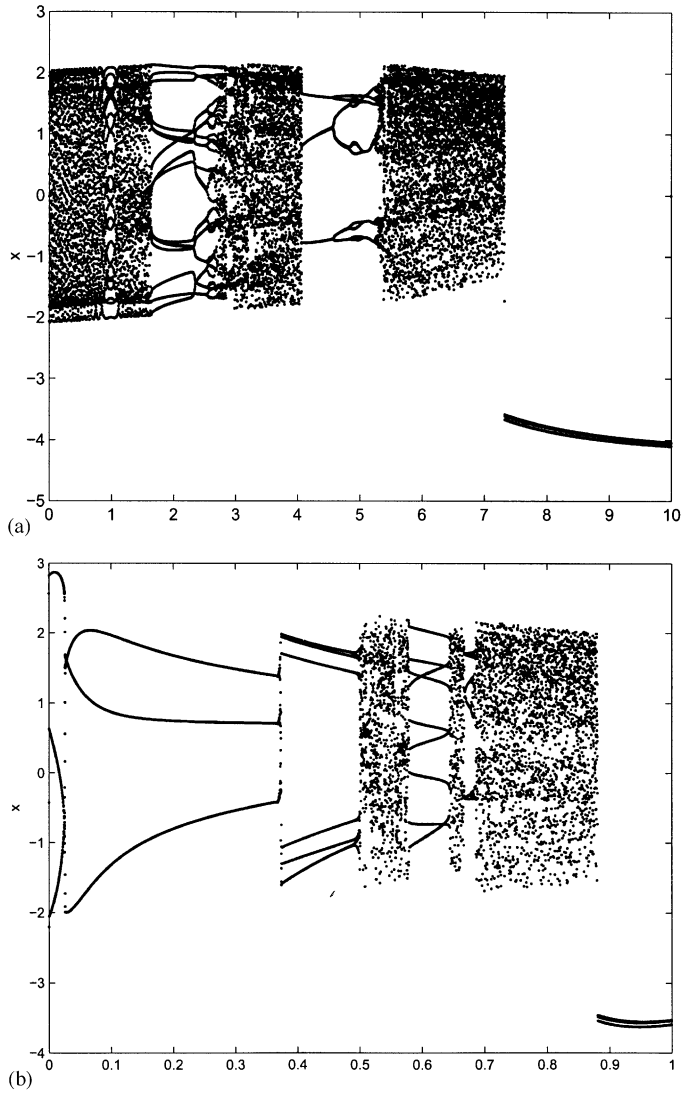

Fig. 1. Bifurcation diagram for $\mu = 0.2$, $\omega_0 = v = 1$, $\omega = 3$, $f = 0.48$, $\alpha = \beta = 0$, (a) $\lambda = 0.8$ and (b) $g = 6.2$.

to the previous case. The scenario so described is repeated once again and the system finally settles into a period-2 motion.

The bifurcation diagram of Fig. 1(b), where λ is varied in the range $0 < \lambda < 1$, is contrary to that of Fig. 1(a). Between the λ intervals, all trajectories lead to an invariant torus, where periodic orbits (3, 6 and 9-periods) are bounded by chaotic intervals until periodic movement occurs. Indeed, it is noticed that for $0 < \lambda < 0.5$, the system displays periodic behaviour (period-3 motion) which abruptly bifurcates into a period-6 at $\lambda \approx 0.375$. In the half-right interval, i.e., $0.5 \leqslant \lambda \leqslant 1$, the pattern of evolution of the system's dynamics is the same as that of Fig. 1(a). That is, chaotic and periodic behaviours succeed each other with a period-2 state as the final behaviour of the system.

It is interesting to note that while the width of the interval of regular behaviour is relatively increasing with the increase of g (in Fig. 1(a)), it actually diminishes when λ is increased.

The second indicator is the largest Lyapunov exponent (denoted L_{max}) computed from the variational equation

$$d\ddot{x} - \mu(1 - x^2)\, d\dot{x} + 2\mu x\dot{x}\, dx + \omega_0^2\, dx + 3\lambda x^2\, dx = 0$$

obtained by linearizing Eqs. (1)–(2) around solution x. $dx, d\dot{x}$ and $d\ddot{x}$ are the variations of x, $\dot{x}$ and, $\ddot{x}$ respectively. The largest Lyapunov exponent can be defined as

$$L_{max} = \lim_{t\to\infty}\left[\frac{\ln\sqrt{dx^2 + d\dot{x}^2}}{t}\right].$$

The signs of the Lyapunov exponents provide a qualitative picture of a system dynamics. The criteria are $L_{max} > 0$ (chaotic) and $L_{max} \leqslant 0$ (regular motion). Fig. 2 presents the Lyapunov exponent as a function of the amplitude of the second external force g. It is clear that the system returns to regular motion when the value of g is presented at a certain interval.

Another mechanism leading to chaotic behaviour due to the effects of the second external force is the torus breakdown by loss of smoothness illustrated in Poincaré maps. The torus of Fig. 3(a), the form of which is approximately a circle, is obtained for $g = 0$; the corresponding Lyapunov exponent is $L_{max} = 0$. For $g = 3$, the shape of this torus begins to deform with the appearance of three pikes (see Fig. 3(b)). The loss of smoothness is already noticeable although the system remains non-chaotic. Increasing the amplitude of the second component of the external force to $g = 4$ accentuates the torus loss of smoothness by producing a fractal geometric shape, and thus the chaotic behaviour of the system. This is depicted in Fig. 3(c). Note that for this value of g, the

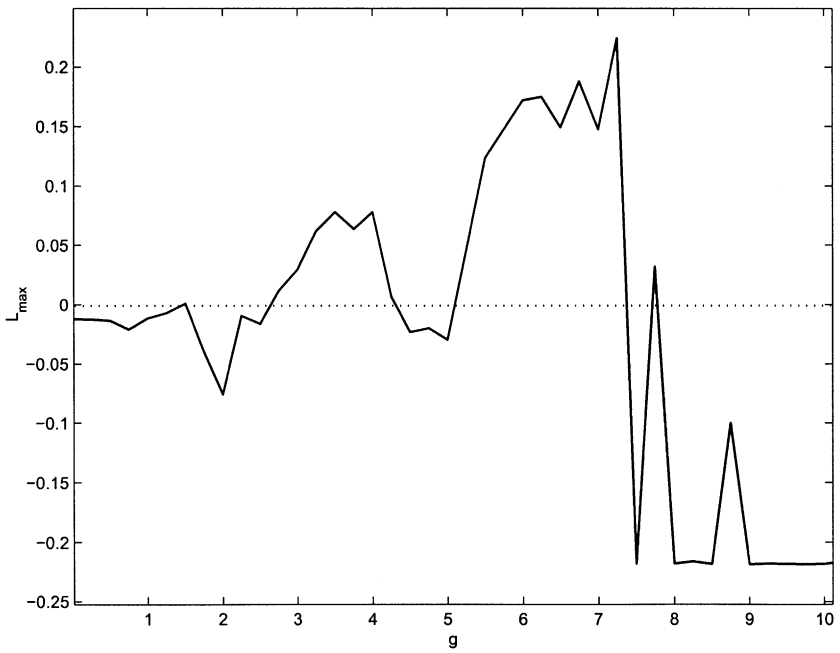

Fig. 2. The maximal Lyapunov exponents against g corresponding to the bifurcation diagram of Fig. 1(a).

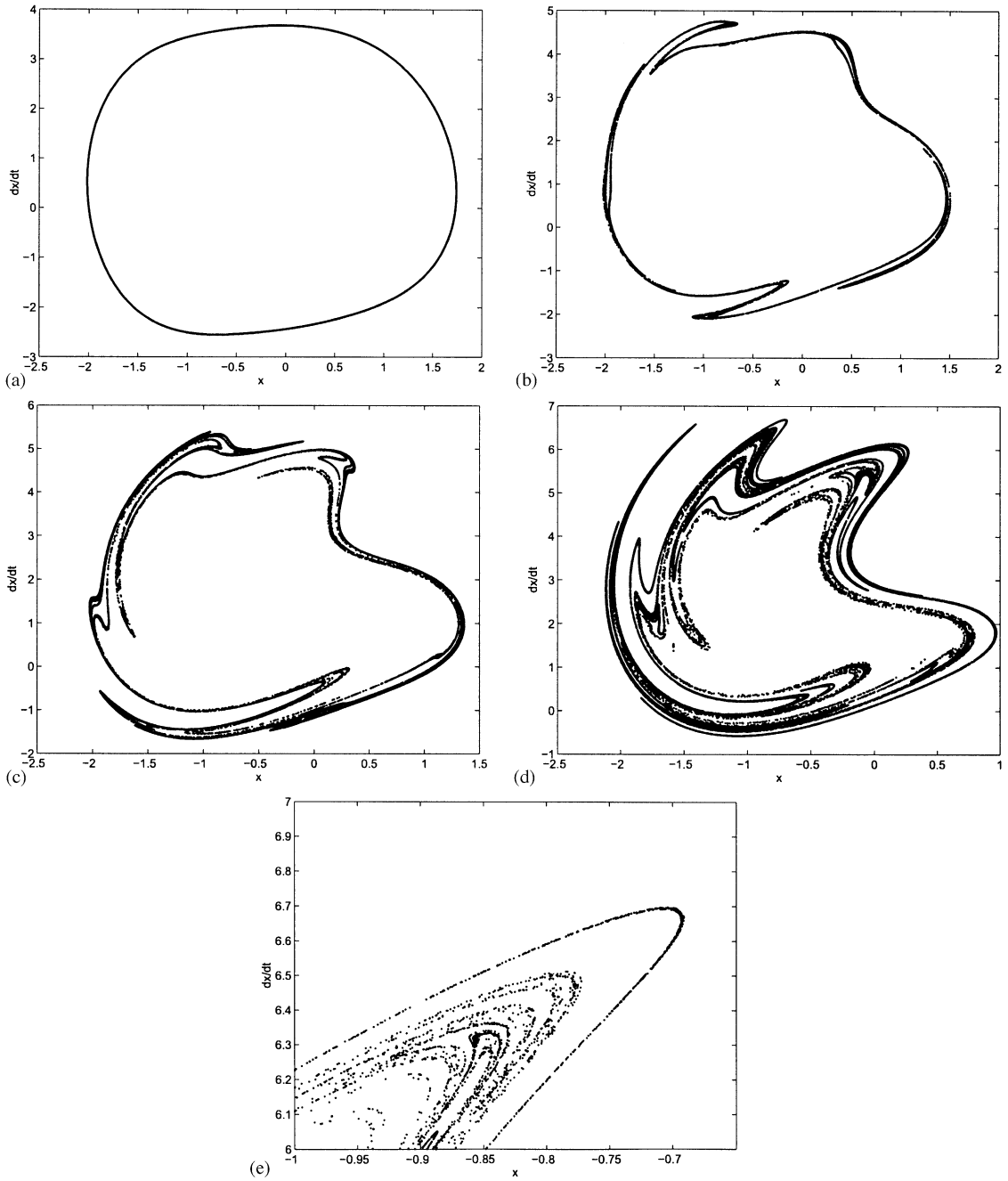

Fig. 3. Poincaré maps; for $\mu = 0.2$, $\omega_0 = v = 1$, $\omega = 3$, $f = 0.48$, $\alpha = \beta = 0$, $\lambda = 0.8$. (a) $g = 0$; (b) $g = 3$; (c) $g = 4$; (d) $g = 6.2$; (e) zoom of (*d*).

maximal Lyapunov exponent is found to be $L_{max} = 0.097$. At last, when $g = 6.2$ ($L_{max} = 0.19$), a nice strange chaotic attractor is shown in Fig. 3(d). From Fig. 3(e), one can easily see that this attractor consists to a number of parallel curves. Such a mechanism of transition to chaos via breaking of tori and formation of attracting homoclinic structure has also been observed in Refs. [4,8].

3. Chaos control

As derived in Section 2, the DVP oscillator presents very complicated dynamics such as coexistence of chaotic attractors with periodic orbit. In practical applications, it is desirable to induce regular dynamics in DVP oscillator to avoid fracture and degradation of the mechanism parts. Persistent external perturbations represented by the time-functionalities in Eq. (2) lead to errors and lag position tracking. To avoid these undesirable dynamical effects, it is necessary to introduce some control actions in the system. However, the practical chaotic systems may contain many types of uncertainties. These uncertainties may cause chaotic perturbations to originally regular behaviour, or induce additional chaos in originally chaotic but known behaviour, generating unknown chaotic motion. In this case, it would be desirable to have a feedback scheme to achieve control in spite of the system's uncertainties.

The purpose of this section, is essentially to develop a robust input–output linearization feedback scheme for controlling a chaotic second order system such as DVP equation (1)–(2) to an appropriate reference signal. It is recalled that DVP's equation (1)–(2) describes a specific non-linear self-excited circuit or a pendulum moving in a non-linear viscous medium and is in controlled form given by

$$\ddot{x} - \mu(1 - x^2)\dot{x} + \omega_0^2 x + \lambda x^3 = f\cos(vt + \alpha) + g\cos(\omega t + \beta) + u. \tag{3}$$

The control u is added in order to guide the chaotic dynamics to meet the specific requirements. It is assumed that uncertainties such as modelling errors, noisy measurements, parameter variations, and time delays are present in the model. The authors are interested in driving the state x to an appropriate defined reference signal x_d. This issue is widely known as the tracking problem in the control community.

The control objective is to solve the following tracking problem: for any bounded reference trajectory x_d whose derivatives $\dot{x}_d$ and $\ddot{x}_d$ are bounded and piecewise continuous on $[0, \infty)$, design a feedback controller $u(t, x, \dot{x})$ that forces the output $y = x$ to track x_d exponentially as $t \to T$ for any initial time instant $t_0 \geqslant 0$ and initial conditions $(x(0), \dot{x}(0)) \in \mathbb{R}^2$, despite modelling errors, parameter variations and time delays in the actuators.

3.1. Feedback stabilization under uncertain vector field

Here the detailed design procedure of the feedback control law u is described with detailed explanations. The main idea behind the proposal is, departing from the uncertain system, to construct an extended non-linear system which should be dynamically equivalent to the canonical representation. In this way, the system's uncertainties are lumped into a non-linear function, which is rewritten into the extended non-linear system as a state variable. After, an observer can be constructed to get an estimated value of the lumping non-linear function via the augmented state variable.

First, some basic notions about exponential stability are recalled.

Consider a non-linear system $\dot{\chi} = h(\chi)$, with $\chi \in \mathbb{R}^n$ and h being locally Lipschitz in χ. Assume that $h(0) = 0$. The system is said to be globally exponentially stable (for short, GES) at the equilibrium $\chi = 0$ if there exists a Lyapunov function V and three positive constants κ_1, κ_2 and κ_3 such that

$$\kappa_1 \|\chi\|^2 \leqslant V(\chi) \leqslant \kappa_2 \|\chi\|^2,$$

and

$$\dot{V}(\chi) = \frac{\partial V}{\partial \chi} h(\chi) \leqslant -\kappa_3 V(\chi).$$

In this way, there exist two positive constants γ and ρ such that the solutions $\chi(t)$ satisfy

$$\|\chi(t)\| \leqslant \gamma e^{-\rho(t-t_0)}, \quad \forall t \geqslant t_0 \geqslant 0. \tag{4}$$

Now let $x = x_1$ and $\dot{x} = x_2$ be defined. In this way, dynamics (3) become

$$\begin{cases} \dot{x}_1 = x_2, \\ \dot{x}_2 = \Theta(x_1, x_2, t) + u, \end{cases} \tag{5}$$

where

$$\Theta(x_1, x_2, t) = \mu(1 - x_1^2)x_2 - \omega_0^2 x_1 - \lambda x_1^3 + f\cos(vt + \alpha) + g\cos(\omega t + \beta)$$

is a smooth non-linear function. In this paper, it is shown that the property of GES is achievable for the DVP system and, moreover, ρ in Eq. (4) can be assigned arbitrarily with the aid of a non-linear observer-based output feedback controller.

In order to design a control law satisfying the control objective stated above, assume the following.

Assumption 1. The output (measurement) of the system is $y = x_1$.

Assumption 2. $\Theta(x_1, x_2, t)$ is unknown function.

Assumption 1 is realistic because in most cases only the position is available for feedback. Although the time derivative of the position can be obtained by means of encoders, the procedure is very sensitive to noisy measurements. Concerning Assumption 2, it is claimed that it is a general and practical situation because the term $\Theta(.)$ involves the uncertainties in the system. The sources of such uncertainties could be parameter mismatching, unknown initial conditions and time delays in the actuators. Hence, the non-linear function $\Theta(x_1, x_2, t)$ is uncertain and it is clear that it cannot be directly used in a linearizing-type feedback.

The idea of dealing with the uncertain term $\Theta(x_1, x_2, t)$ is to lump it into a new state v. Then, system (5) can be rewritten as the following (extended dynamically equivalent) system:

$$\begin{cases} \dot{x}_1 = x_2, \\ \dot{x}_2 = v + u, \\ \dot{v} = \Xi(x_1, x_2, v, u, t), \end{cases} \tag{6}$$

where

$$\Xi(x_1, x_2, v, u, t) = x_2\partial_1\Theta(x_1, x_2, t) + (v + u)\partial_2\Theta(x_1, x_2, t) + \partial_t\Theta(x_1, x_2, t),$$

with $\partial_k\Theta(x_1, x_2, t) = \partial\Theta(x_1, x_2, t)/\partial x_k, k = 1, 2$ and $\partial_t\Theta(x_1, x_2, t) = \partial\Theta(x_1, x_2, t)/\partial t$.

Or in a matrix equation form as

$$\begin{cases} \dot{\mathbf{X}} = \mathscr{A}\mathbf{X} + \mathbf{B}(v + u), \\ \dot{v} = \Xi(X, v, u, t), \end{cases} \tag{7}$$

where $\mathbf{X} = (x_1, x_2)^{\mathrm{T}}$,

$$\mathscr{A} = \begin{bmatrix} 0 & 1 \\ 0 & 0 \end{bmatrix} \quad \text{and} \quad \mathbf{B} = \begin{bmatrix} 0 \\ 1 \end{bmatrix}.$$

System (6) has the following properties:

1. Under the vector field defined in system (6), the set $M = \{(x_1, x_2, v) \in \mathbb{R}^3 : \psi(x_1, x_2, v, t) = v - \Theta(x_1, x_2, t)\}$ is an invariant three-dimensional manifold. In order to prove this property, it suffices to show that $\mathrm{d}\psi(x_1, x_2, v, t)/\mathrm{d}t = 0$ for all $t \geqslant 0$ or equivalently $x_2\partial_1\Psi(x_1, x_2, v, t) + (v + u)\partial_2\Psi(x_1, x_2, v, t) + \dot{v}\partial_v\Psi(x_1, x_2, v, t) + \partial_t\psi(x_1, x_2, v, t) = 0$. This is automatically satisfied because $\partial_v\Psi(x_1, x_2, v, t) = 1$ and $\dot{v} = -x_2\partial_1\Psi(x_1, x_2, v, t) - (v + u)\partial_2\Psi(x_1, x_2, v, t) - \partial_t\psi(x_1, x_2, v, t)$.
2. For all $u \in \mathbb{R}$, system (6) has the same solution as system (5) module $\pi : (x_1, x_2, v) \to (x_1, x_2)$, if $v(0) = \Theta(x_1(0), x_2(0), 0)$. That is if $\Psi(x_1(0), x_2(0), v(0), 0)$ is a solution of the system (6), then $\pi \cdot \Psi(x_1(0), x_2(0), v(0), 0)$ is a solution of the system (5). To prove this property let the last equation of Eq. (6) be integrated to get (considering the invariance of $\Psi(x_1, x_2, v, t)$ given by the first property) $v(t) = \Theta(x_1, x_2, t) + c$, where c is an integration constant. The condition $\Psi(x_1, x_2, v, t) = 0$ implies that $v(0) = \Theta(x_1(0), x_2(0), 0)$ and hence $c = 0$. Then, when $v(t)$ is back-substituted in the second equation of Eq. (6), the solution of system (5) is obtained. Consequently, $\pi \cdot \Psi_t(x_1(0), x_2(0), v(0), 0) = \Psi_t(x_1(0), x_2(0), 0)$ where $\Psi_t(x_1(0), x_2(0), v(0), 0) = \Psi_t(x_1(0), x_2(0), 0)$ is the solution of system (6) with initial conditions $(x_1(0), x_2(0), \eta(0))$ and $\Psi_t(x_1(0), x_2(0), 0)$ denotes the solution of system (5) with initial conditions $(x_1(0), x_2(0))$.
3. The transformed system (6) is a fully linearizable non-linear system. In addition, system (6) is in a cascade form. This means that when action is taken to achieve $\lim X \to X_d$, the part $\Xi(X, v, u, t) \to \Xi(X_d, v, u, t) \to X_d$ asymptotically for the so-called cascade character [16].

For any positive real number θ, define

$$\mathbf{\Delta}_\theta = \begin{bmatrix} \theta^{-1} & 0 \\ 0 & \theta^{-2} \end{bmatrix},$$

$\forall \mathbf{K} \in \mathbb{R}^{1\times 2}$, there exists $\tilde{\mathbf{K}} \in \mathbb{R}^{1\times 2}$ such that

$$\mathbf{B}\tilde{\mathbf{K}} = \theta\mathbf{\Delta}_\theta^{-1}\mathbf{B}\mathbf{K}\mathbf{\Delta}_\theta,$$

and $\tilde{\mathbf{K}}$ is given by the following formula:

$$\tilde{\mathbf{K}} = \theta\mathbf{B}^{\mathrm{T}}\mathbf{\Delta}_\theta^{-1}\mathbf{B}\mathbf{K}\mathbf{\Delta}_\theta. \tag{8}$$

The controller is designed as follows

$$u = \dot{x}_{2d}(t) - v + \tilde{\mathbf{K}}\mathbf{e}, \tag{9}$$

where $\tilde{\mathbf{K}}$ is defined as in Eq. (8) and $\mathbf{K}$ is such that $(\mathscr{A} + \mathbf{BK})$ has all its eigenvalues with negative real parts and

$$\mathbf{e} = \begin{bmatrix} e_1 \\ e_2 \end{bmatrix} = \begin{bmatrix} x_1 - x_{1d} \\ x_2 - x_{2d} \end{bmatrix},$$

is the tracking error. Substituting Eq. (9) into Eq. (7) and noticing that $\theta\mathbf{\Delta}_\theta^{-1}\mathscr{A}\mathbf{\Delta}_\theta = \mathscr{A}$, it follows that the tracking error-dynamics $\mathbf{e}$ satisfies

$$\begin{cases} \dot{\mathbf{e}} = \theta\mathbf{\Delta}_\theta^{-1}(\mathscr{A} + \mathbf{BK})\mathbf{\Delta}_\theta\mathbf{e}, \\ \dot{\eta} = \Gamma(\mathbf{e}, \eta, u, t), \end{cases} \tag{10}$$

where $\eta = v - v_d$ and $\Gamma(.) = \Xi(x_1, x_2, v, u, t) - \Xi(x_{1d}, x_{2d}, v, u, t)$.

The desired stability properties of the closed-loop system are summarized in the following result.

Theorem 1. *Consider the DVP equation* (6) *in closed loop with the control law* (9). *The closed-loop system* (10) *is GES at the origin, i.e., the solutions* $(\mathbf{e}(t), v(t))$ *satisfy the property* (4).

Proof. Define the Lyapunov function as

$$V(e) = \mathbf{e}^{\mathrm{T}}\mathbf{\Delta}_\theta\mathbf{S}\mathbf{\Delta}_\theta\mathbf{e}, \tag{11}$$

where $\mathbf{S}$ is the symmetric positive definite matrix, solution of the matrix equation

$$(\mathscr{A} + \mathbf{BK})^{\mathrm{T}}\mathbf{S} + \mathbf{S}(\mathscr{A} + \mathbf{BK}) = -\mathbf{I}_{\mathbb{R}^2},$$

with $\mathbf{I}_{\mathbb{R}^2}$ the identity matrix of dimension 2.

Its time derivative along the trajectories of system (10) satisfies

$$\dot{V}(\mathbf{e}) = -\theta\|\mathbf{\Delta}_\theta\mathbf{e}\|^2. \tag{12}$$

Remark that

$$\lambda_{\min}(\mathbf{S})\|\mathbf{\Delta}_\theta\mathbf{e}\|^2 \leqslant V(\mathbf{e}) \leqslant \lambda_{\max}(\mathbf{S})\|\mathbf{\Delta}_\theta\mathbf{e}\|^2,$$

where $\lambda_{\min}(\mathbf{S})$ and $\lambda_{\max}(\mathbf{S})$ are the minimum and the maximum eigenvalues of the matrix $\mathbf{S}$. Hence,

$$\dot{V}(\mathbf{e}) \leqslant \frac{-\theta}{\lambda_{\max}(\mathbf{S})}V(\mathbf{e}).$$

Then one has

$$V(\mathbf{e}) \leqslant V(0)\exp\left\{\frac{-\theta t}{\lambda_{\max}(\mathbf{S})}\right\},$$

which implies that

$$\|\mathbf{\Delta}_\theta \mathbf{e}\| \leqslant \left[\frac{V(\mathbf{e})}{\lambda_{\min}(\mathbf{S})}\right]^{1/2} = \left[\frac{V(0)}{\lambda_{\min}(\mathbf{S})}\right]^{1/2} \exp\left\{\frac{-\theta t}{2\lambda_{\max}(\mathbf{S})}\right\}$$
$$\leqslant \left[\frac{\lambda_{\max}(\mathbf{S})}{\lambda_{\min}(\mathbf{S})}\right]^{1/2} \exp\left\{\frac{-\theta t}{2\lambda_{\max}(\mathbf{S})}\right\}$$

Taking into account that

$$\theta^{-2}\|\mathbf{e}\| \leqslant \|\mathbf{\Delta}_\theta \mathbf{e}\| \leqslant \theta^{-1}\|\mathbf{e}\|,$$

one has

$$\|\mathbf{e}(t)\| \leqslant \left[\frac{\lambda_{\max}(\mathbf{S})}{\lambda_{\min}(\mathbf{S})}\right]^{1/2} \theta\|\mathbf{e}(0)\| \exp\left\{\frac{-\theta t}{2\lambda_{\max}(\mathbf{S})}\right\} \to 0, \tag{13}$$

which implies that for some $T > 0$

$$\lim_{t \to T} x_i(t) = x_{id}(t), \quad i = 1, 2.$$

Convergence of η to zero (or v to v_d) follows from the fact that the closed-loop system is in cascade form [16]. The control dynamics is given by $\dot{u} = \ddot{x}_{2d} - \Xi(x_1, x_2, v, u, t) + \tilde{\mathbf{K}}\dot{\mathbf{e}}$. Since $x_i(t)$, $i = 1, 2$ belong to some chaotic attractor, then $\Theta(x_1, x_2, t)$ and its derivatives $\partial\Theta(x_1, x_2, t)/\partial x_k$, $k = 1, 2$, are bounded. This means that $\Xi(x_1, x_2, v, u, t)$ is a smooth and bounded function. Hence, $\dot{u}$ is also a smooth and bounded function because x_{1d}, $\dot{x}_{1d}$ and $\ddot{x}_{1d}$ are bounded. In addition, since $v = \Theta(x_1, x_2)$, v is bounded. Then since $\eta = v - v_d$, η is bounded. Finally, since $\mathbf{e}(t)$ expontentially converges to zero, $\eta(t)$ also converges to zero and this achieves the proof. □

The θ-parametrization of the feedback control law (9) provides a simple tuning procedure. In fact, since $\|\mathbf{e}(t)\| \leqslant \gamma \exp\{-(\theta t/2\lambda_{\max}(\mathbf{S}))\}$, $\forall t \geqslant T$, the larger the value of θ, the faster the convergence of the error $\mathbf{e}_i = x_i - x_{id}$, $i = 1, 2$.

It will now be proved that the convergence of $\mathbf{e}(t)$ to the origin takes place at a finite time T. One way to compute the control time T is to follow the time trajectory of system (13). In this case, the control objective is achieved when the error $\mathbf{e}(t)$ is less than a precision, i.e., it obeys the following condition:

$$|\mathbf{e}(t)| \leqslant h, \quad t \geqslant T, \tag{14}$$

where h is the control precision. From Eq. (13), a simple algebraic calculations yields

$$T = \frac{2\lambda_{\max}(\mathbf{S})}{\theta} \ln \frac{\theta\|\mathbf{e}_0\|}{h} \sqrt{\frac{\lambda_{\max}(\mathbf{S})}{\lambda_{\min}(\mathbf{S})}}, \tag{15}$$

where $\mathbf{e}_0 = \mathbf{e}(0)$ is the initial state of $\mathbf{e}(t)$. One can notice that T increases logarithmically with the initial state norm $\|\mathbf{e}_0\|$, but decreases with θ.

From Eq. (9), it is known that the control law is not physically realizable because it requires the measurements of the states x_i, $i = 1, 2$ and the uncertain term $\Theta(.)$. So a special way must be to estimate $\Theta(.)$ and x_i, $i = 1, 2$ based on the available signal $y = x_1$ to make the feedback control law (9) physically realizable. By using the results reported in Ref. [14], an observer can be

constructed to get an estimated value of the lumping non-linear function via the augmented state variable. Based on extended state observer, the following high-gain estimator can be obtained:

$$\begin{cases} \dot{\hat{x}}_1 = \hat{x}_2 - \theta E_1(\hat{x}_1 - x_1), \\ \dot{\hat{x}}_2 = \hat{v} + u - \theta^2 E_2(\hat{x}_1 - x_1), \\ \dot{\hat{v}} = -\theta^3 E_3(\hat{x}_1 - x_1), \end{cases} \tag{16}$$

where $(\hat{x}_1, \hat{x}_2, \hat{v})$ are estimated values of (x_1, x_2, v), respectively; and E_1, E_2 and E_3 are estimation constants which are chosen in such a way that the polynomial $s^3 + E_1 s^2 + E_2 s + E_3 = 0$ has all its roots in the open half-hand complex.

Combining systems (6) and (16), the dynamics of the estimation error $\tilde{\mathbf{e}}_i = \theta^{2-i}\hat{x}_i - x_i$, $i = 0, 1$ and $\tilde{\mathbf{e}}_3 = \hat{v} - v$ can be written as follows:

$$\dot{\tilde{\mathbf{e}}} = \theta \mathscr{D}\tilde{\mathbf{e}} + [0, 0, \Xi(x_1, x_2, v, u, t)]^{\mathrm{T}}, \tag{17}$$

where $\tilde{\mathbf{e}} = (\tilde{\mathbf{e}}_1, \tilde{\mathbf{e}}_2, \tilde{\mathbf{e}}_3)^{\mathrm{T}}$ and $\mathscr{D} \in \mathbb{R}^{3\times 3}$ is the companion matrix given by

$$\mathscr{D} = \begin{bmatrix} -E_1 & 1 & 0 \\ -E_2 & 0 & 1 \\ -E_3 & 0 & 0 \end{bmatrix}.$$

Since the trajectories $x_i(t)$, $i = 1, 2$ are contained in a chaotic attractor, hence, $\Xi(x_1, x_2, v, u, t)$ is bounded. Consequently, for any sufficiently large value of the high-gain parameter θ, $\tilde{\mathbf{e}} \to 0$ as $t \to \infty$, which implies that $(\hat{x}_1, \hat{x}_2, \hat{v}) \to (x_1, x_2, v)$.

Thus, the following output-feedback control law is chosen, derived from Eq. (9)

$$u = \dot{x}_{2d}(t) - \hat{v} + \tilde{\mathbf{K}}\hat{\mathbf{e}}. \tag{18}$$

The authors are now ready to state the second result on the global output-feedback control of the DVP equation (6).

Theorem 2. *Consider the DVP equation* (6) *in closed loop with the observer-based output-feedback control law* (16), (18). *The closed-loop system is GES at the origin, i.e., the solutions* ($\mathbf{e}(t)$) *satisfy property* (4) *and the control time becomes*

$$T = \frac{2\lambda_{\max}(\mathbf{S})}{\theta} \ln \frac{\theta \|\hat{\mathbf{e}}_0\|}{h} \sqrt{\frac{\lambda_{\max}(\mathbf{S})}{\lambda_{\min}(\mathbf{S})}}, \tag{19}$$

where $\hat{\mathbf{e}}_0 = \hat{\mathbf{e}}(0)$ *is the initial state of* $\hat{\mathbf{e}}(t)$.

Proof. Since the estimation error $\tilde{\mathbf{e}}$ is globally exponentially stable at zero one has that $\hat{x}_i \to x_i$, $i = 1, 2$ and $\hat{v} \to v$. As a consequence, the feedback control law (18) tends to the linearizing feedback control law given by Eq. (9). Then, control actions counteract the non-linear uncertainties and induce a linear behaviour. □

Notice that the linearizing control law (18) only uses the estimation of the uncertain term $\Theta(x_1, x_2, t)$ (by means $\hat{v}$) and $\hat{x}_i$, $i = 1, 2$. And the dynamical estimator (16) only uses the

measurable state $y = x_1$. So the feedback control law (18) neglects the system uncertainties and is more physically realizable than (9).

Note that since $\Theta(x_1, x_2, t)$ is uncertain, the function $\Xi(x_1, x_2, v, u, t)$ is correspondingly unknown. Thus, such a term was not used in the construction of the observer (16). This feature yields a low-order parametrization (only a tuning parameter is required) to the dynamic compensator of the adaptive strategy. Note also that the order of the proposed controller does not increase with the number of parameters because it does not require information about system parameters. This is an advantage with respect to previous control schemes.

Feedback control based on high-gain observers can induce undesirable dynamics effects such as the so-called peaking phenomenon [17]. This phenomenon leads to closed-loop instabilities which are represented by time-finite escapes and large overshooting. To diminish the effect of these instabilities, the control law (18) can be modified by means of [18]

$$u = Sat\{\dot{x}_{2d}(t) - \hat{v} + \tilde{\mathbf{K}}\hat{\mathbf{e}}\}, \tag{20}$$

where

$$Sat\{.\}\begin{cases} = U_{\max}, & \text{if } u > U_{\max}, \\ = \dot{x}_{2d}(t) - \hat{v} + \tilde{\mathbf{K}}\hat{\mathbf{e}}, & \text{if } -U_{\max} \leqslant u \leqslant U_{\max}, \\ = -U_{\max}, & \text{if } u < -U_{\max}. \end{cases}$$

3.2. Simulation results

Computer simulation is used to verify the performance of the proposed controller. Consider system (3) with the initial condition $(x_1(0), x_2(0)) = (0.5, 0)$ and the observer (16) with $(\hat{x}_1(0), \hat{x}_2(0), \hat{v}(0)) = (0.6, 0, 7.1)$. Without the control u, the DVP oscillator is known to generate a chaotic phenomenon when the system parameters are set at values $\mu = 0.2$, $\omega_0 = 1$, $f = 0.48$, $v = 1$, $\omega = 3$, $g = 6.2$ and $\lambda = 0.8$ (see Fig. 3(d)). The output reference state is set as $y_d = x_{1d}(t) = \sin \omega t$. Hence, $x_{2d}(t) = \omega \cos \omega t$. The control gains were chosen as $K_1 = -1$ and $K_2 = -2$, such that $(\mathscr{A} + \mathbf{BK})$ has all its roots located at -1. The values of the estimator parameter were chosen as $E_1 = 3$, $E_2 = 3$ and $E_3 = 1$. Then the eigenvalues of the polynomial $s^3 + E_1 s^2 + E_2 s + E_3 = 0$ are located at -1. Controller (18) is activated at $t = 20$ s.

Fig. 4(a) shows the time needed to achieve tracking as a function of θ for $h = 10^{-4}$, while Fig. 4(b) presents the control time as a function of $\|\hat{\mathbf{e}}(0)\|$ for $h = 10^{-4}$ and $\theta = 20$. Fig. 5 shows the position x_1 and the velocity x_2 time evolutions before and after the controller is activated. The free parameter θ was taken as $\theta = 20$. The figures show that the linearizing-like control proposed in this section can successfully bring the state to the reference $(x_{1d}(t), x_{2d}(t))$ in about 1 s. Note that when the control is turned, the velocity has a sharp peak. This is due to the fact that the control command is acting only on the state x_2 and the feedback scheme is based on high-gain feedback, which can induce undesirable dynamics effect such as the peaking phenomenon. The effect of the sharp peak in the output can be diminished by means of a saturation function of the feedback controller. When $U_{\max} = 15$ was arbitrarily chosen, the performance of the satured version of the controller is presented in Fig. 6.

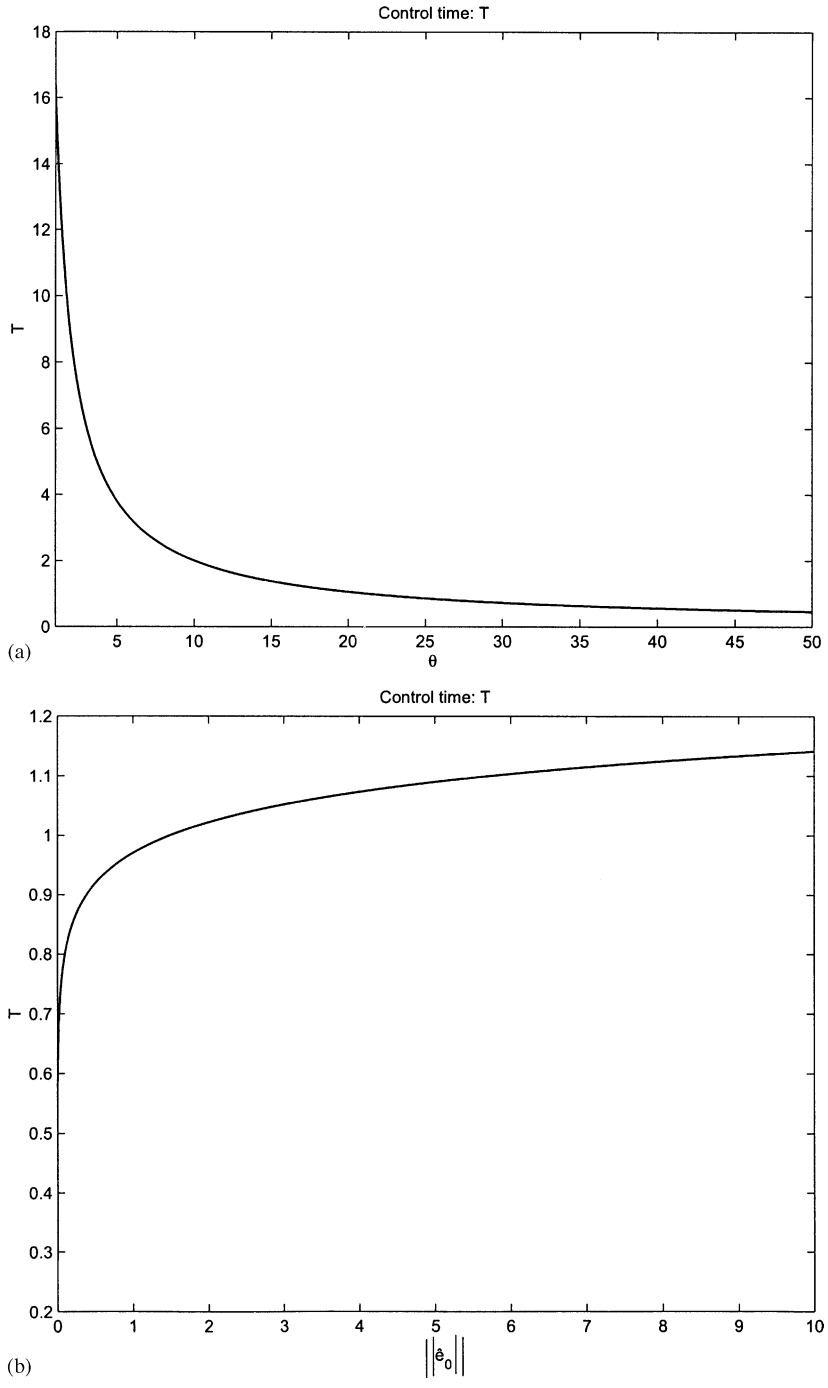

Fig. 4. Control time for $h = 10^{-4}$: (a) as a function θ; (b) as a function of the initial state norm $\|\hat{\mathbf{e}}_0\|$ when $\theta = 20$.

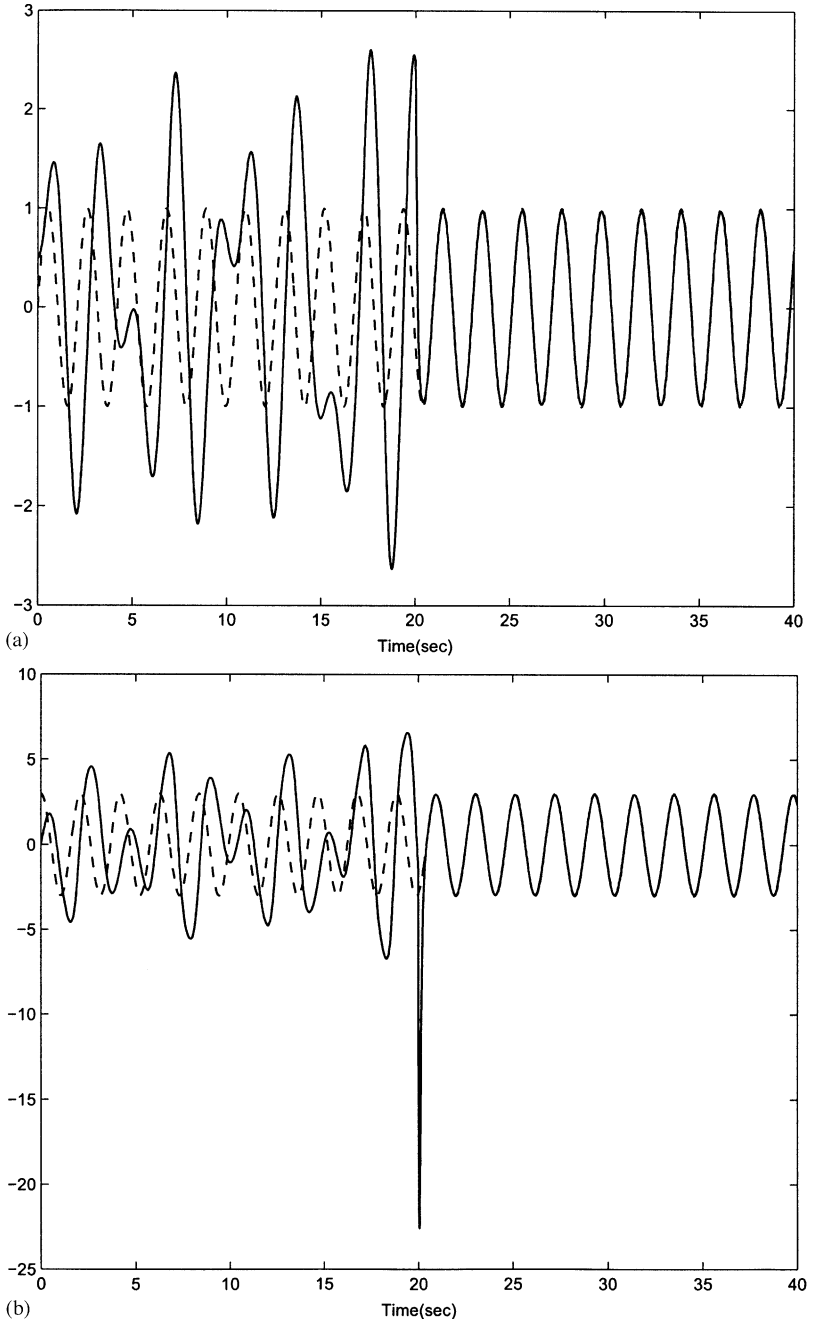

Fig. 5. Time response of DVP's equation: (a) x_1 component (—) together with its desired value (- - -); (b) $\dot{x}_2$ component (—) together with its desired value (- - -) when $\theta = 20$.

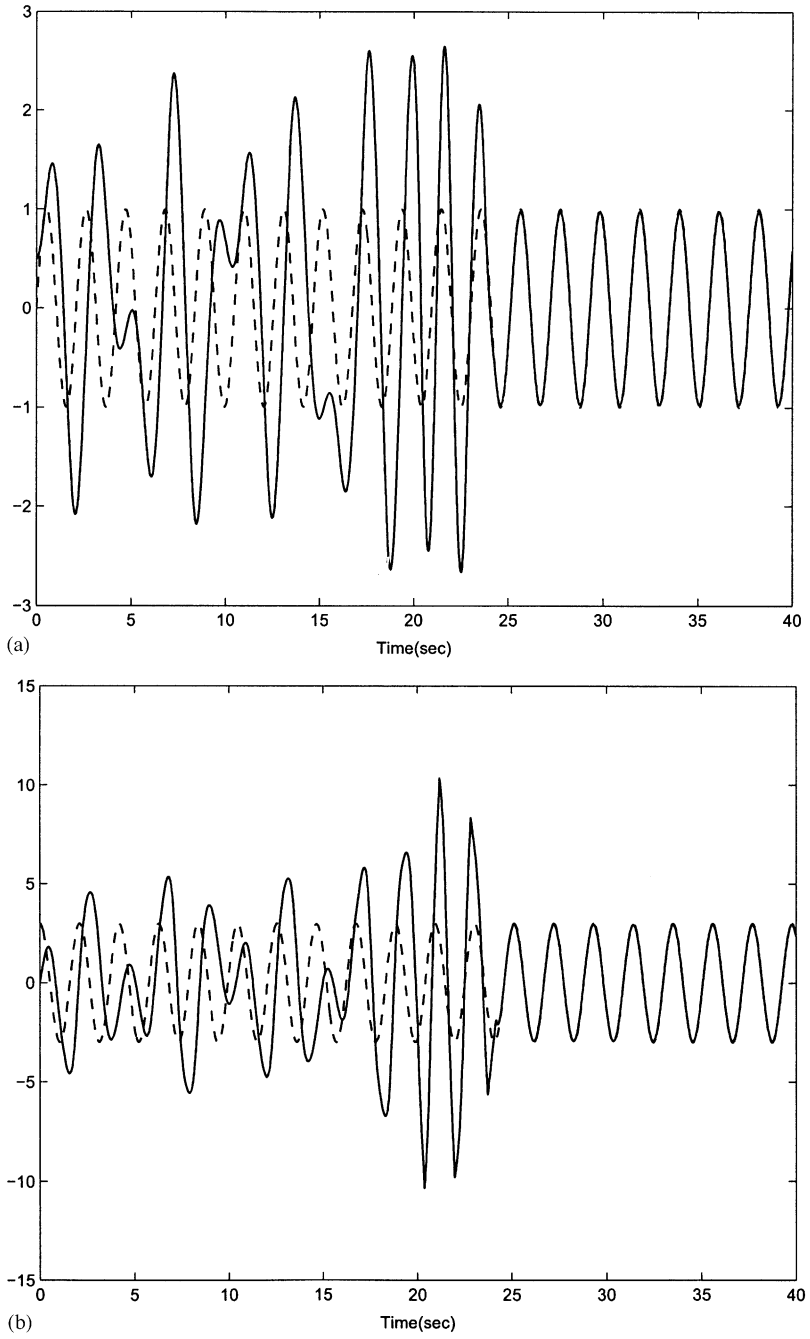

Fig. 6. Performance of the saturated version of the control input, $\theta = 20$: (a) x_1 component (—) together with its desired value (- - -); (b) $\dot{x}_2$ component (—) together with its desired value (- - -).

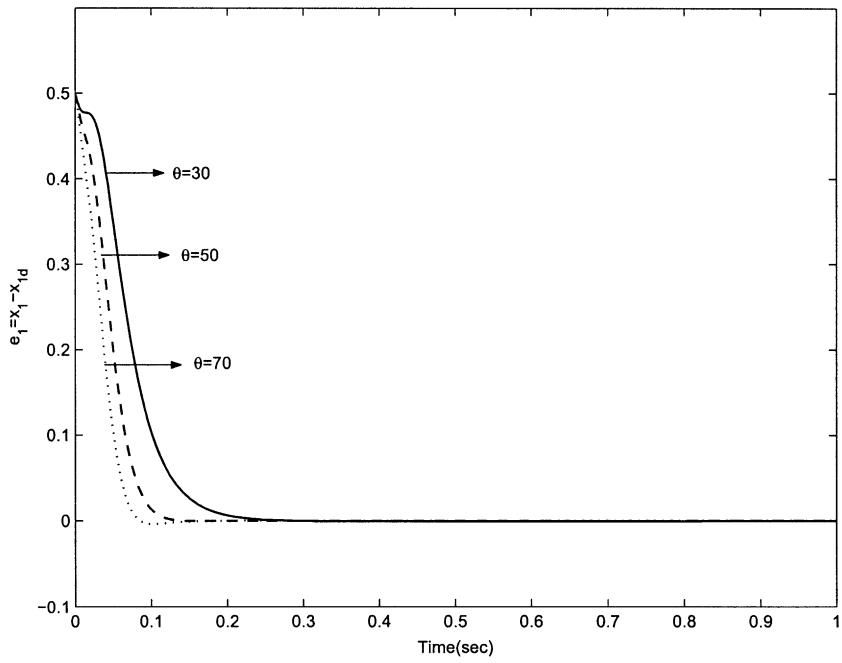

Fig. 7. Tracking error $\mathbf{e}_1 = x_1 - x_{1d}$ for three different values of the high-gain parameter θ.

To further verify the effectiveness of the proposed feedback strategy, the robust output feedback controller (20) is simulated with different values of the parameter θ. Fig. 7 shows the tracking error $\mathbf{e}_1 = x_1 - x_{1d}$ for three different values of θ. As expected, the larger the value of θ, the faster the convergence.

4. Conclusion

The periodic and chaotic motions of the non-autonomous DVP system with two external periodic forces are obtained by numerical methods such as bifurcation diagram, Lyapunov exponent and Poincaré map. Many chaotic phenomena have been displayed in bifurcation diagrams. More information on the behaviour of the periodic and chaotic motions can be found in Poincaré maps.

A control scheme for chaos suppression has been presented. The main idea is to lump the uncertainties in a non-linear function which can be interpreted as an augmented state in a dynamically equivalent DVP oscillator. A state estimator provides an estimated value of the augmented state and, consequently, of the uncertainties. Thus, the controller comprises two parts: a state observer and a linearizing-like control law. The feedback controller was given in terms of a high-gain parameter, which can be easily turned to trade off between stability (convergence). In later work, it is hoped that the method will be useful for developing a practical synchronized chaotic DVP oscillator.

Acknowledgements

The authors are grateful to Professors G. Chen and R. Femat for supplying them with consistent bibliographies on the domain. F.M. Moukam Kakmeni also acknowledges the support from the Abdus Salam International Centre for Theoretical Physics (ICTP) where a part of this work was done during his 2002 participation at the "School and Conference on Spatiotemporal Chaos".

References

[1] J. Guckenheimer, P. Holmes, *Nonlinear Oscillation and Bifurcation of Vector Fields*, Springer, New York, 1993.
[2] E. Atlee Jackson, *Perspectives of Nonlinear Dynamics*, Cambridge University Press, New York, 1991.
[3] M. Lakshmanan, K. Murali, *Chaos in Nonlinear Oscillators: Controlling and Synchronization*, World Scientific, Singapore, 1996.
[4] A.K. Kozlov, M.M. Sushchik, Ya.I. Molkov, A.S. Kuznetsov, Bistable phase synchronization and chaos in system of coupled Van der Pol–Duffing oscillators, *International Journal of Bifurcation and Chaos* 9 (1999) 2271–2277.
[5] W. Szemplińska-Stupnicka, J. Rudowski, Neimark bifurcation, almost-periodicity and chaos in the forced van der Pol–Duffing system in the neighbourhood of the principal resonance, *Physics Letters A* 192 (1994) 201–206.
[6] A. Venkalesam, M. Lakshmanan, Bifurcation and chaos in the double well Duffing–van der Pol oscillator: numerical and analytical studies, *Physical Review E* 56 (1997) 6321–6330.
[7] B. van der Pol, Forced oscillations in a circuit with nonlinear resistance (receptance with reactive triode), *London, Edinburgh, and Dublin Philosophical Magazine* 7 (1927) 65–80.
[8] Z.M. Ge, T.N. Lin, Chaos, chaos control and synchronization of a gyrostat system, *Journal of Sound and Vibration* 251 (2002) 519–542.
[9] K. Yagasaki, Chaotic motions near homoclinic manifold and resonant toris in quasiperiodic perturbations of planar Hamiltonian systems, *Physica D* 69 (1993) 269–322.
[10] K. Yagasaki, Homoclinic motion and chaos in the quasiperiodically forced Van der Pol–Duffing oscillator with single well potential, *Proceedings of the Royal Society of London A* 445 (1994) 597–617.
[11] E. Ott, C. Grebogi, J. Yorke, Controlling chaos, *Physica Review E* 64 (1990) 1196–1199.
[12] W.J. Freeman, The physiology of perception, *Scientific American* (1991) 78–85.
[13] A. Iggidr, G. Sallet, Exponential stabilization of nonlinear systems by an estimated state feedback, *Proceedings of the Second European Control Conference EEC'93*, *Groningen*, *The Netherlands*, 1993, pp. 2015–2018.
[14] A. Teel, L. Praly, Tool for semiglobal stabilization by partial state and output feedback, *SIAM Journal of Control and Optimization* 33 (1991) 424–431.
[15] F.K. Moukam, S. Bowong, C. Tchawoua, Exponential stabilization of two nonlinearly coupled oscillators by an estimated state feedback, *Physica Scripta* 66 (2002) 7–15.
[16] R. Femat, J. Alvarez-Ramirez, B. Castillo-Toledo, J. Gonzalez, On robust chaos suppression in a class of nondriven oscillators: application to the Chua's circuit, *IEEE Circuits and Systems I: Fundamental Theory and Applications* 46 1150–1152.
[17] L.O. Chua, T. Yang, G.Q. Zhong, C.W. Wu, Adaptive synchronization of Chua oscillations, *International Journal of Bifurcation and Chaos* 6 (1996).
[18] H.J. Sussman, P.V. Kokotovic, The peaking phenomenon and the global stabilization of nonlinear systems, *IEEE Transactions on Automatic Control* 36 (1991) 461–472.